The effects of external loading on low displacement wear rates of unlubricated steels

Luke Blades[a,b], David Hills[b], David Nowell[b,c], Ken E Evans[a], Chris Smith[a]

[a] *College of Engineering, Mathematics and Physical Sciences, University of Exeter, Exeter EX4 4QF, UK*
[b] *Department of Engineering Science, University of Oxford, Parks Road, Oxford, OX1 3PJ, UK*
[c] *Department of Mechanical Engineering, Imperial College London, London, SW7 2AZ, UK*

Abstract

Whilst contact loading is known to affect wear, the general stress field is rarely considered. Steel fretting (and low amplitude reciprocating) wear contacts typically develop through a transient regime and wear by multiple mechanisms. It is expected that if these mechanisms were controlled by plasticity or fatigue, the wear rate would be altered by external stresses. Whether or not these stresses must be accounted for is an important consideration. This paper assesses the sensitivity of wear rate to external stresses, experimentally. An apparatus was designed to apply external loads to fretting wear contacts. The wear rates throughout the tests were insensitive to changes in external load, indicating that wear models need only model stresses due to contact loading, and external loads can be disregarded.

Keywords: Fretting, Wear, External loading, Steel

1. Introduction

1.1. Fretting wear and external stresses

Wear problems are often overcome through the use of large bearing surfaces to lower pressure, and through the use of lubricants to lower the coefficient of friction. Fretting wear is a challenge in mechanical design as it can occur between components which are in nominally static contact, preventing lubrication. The range of amplitudes within which fretting wear mechanisms operate is not universally agreed, however a common figure is around 300 µm [1]. This absolute displacement is not important, but rather the displacement relative to the contact size, as this determines the ease of debris egress. Often, wearing components will be subject not only to contact loads but also to external loading. A clarification of this distinction is given in figure 1. Classical wear models such as the Archard law [2], acknowledge the influence of normal load in a wearing contact, but not the effects of the more general stress field, in particular the impact of stress acting parallel with the free surface. Figure 1 shows the loads required to define a partially stuck and incomplete contact. The contacts studied here are fully sliding albeit of small displacement, so the components σ_A and σ_B will not have an effect on the tractions as they do in contacts under partially stuck

conditions [3]. The question addressed here, is whether the additional stress in the wearing material, resulting from these loads, has any effect on the wear rate.

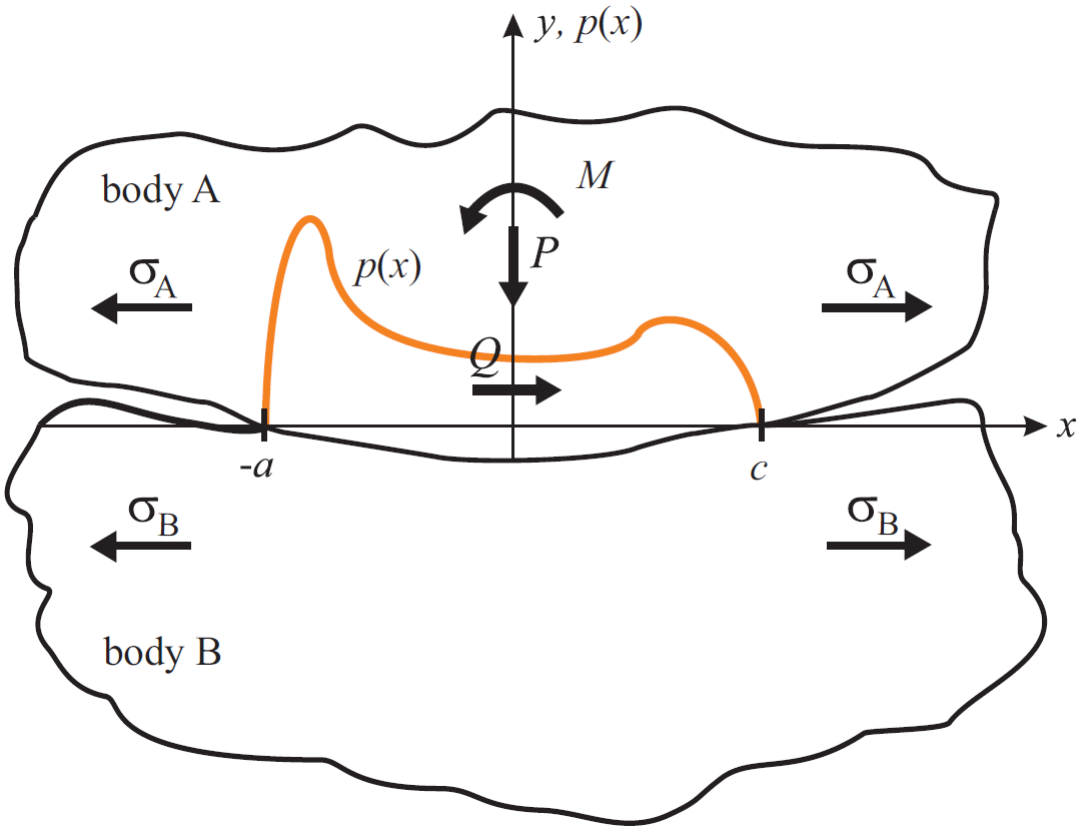

Figure 1: A diagram showing the load components required to define a partially stuck, incomplete contact [3].

Damage in metal components is usually attributed to one of the following:

1. Plastic flow
2. Brittle fracture
3. Chemical change / corrosion

If the dominant wear mechanisms were plasticity driven, then it is reasonable to assume that wear rate ought to be controlled, *not* by the contact pressure alone, but by a yield parameter. So if we assume that von-Mises' criterion applies, the non-traction component of stress, for example (the direct stresses parallel with the free surface) ought also to contribute to the wear rate. Further, if the wear particle nucleation and early development were *crack related*, then surface tension ought also to have a strong effect on rates of wear, just as it would if it were causing the growth of fatigue cracks [4]. We conclude that if *either* of these mechanisms is responsible, fundamentally, for the generation of wear particles, then tension (or compression) parallel with the free surface might be expected to change wear rate. These

remarks apply whether the tension is present along the direction of sliding, or transversely, or both. This hypothesis is explored experimentally in this paper.

1.2. Surface treatment induced residual stresses

Stresses parallel with the free surface might originate either from externally applied loads, or from the presence of self-equilibrating residual stresses. These might arise because of manufacturing processes, or because the surface has been subjected to some surface treatment which gives rise to residual stresses (peening or electro-plating, for example). Lin et al [5] showed that residual compressive stresses (700 MPa) in treated steel *reduced* abrasive wear. Much of the previous work, such as that cited here and that reviewed in [5], on the effects of residual stress on wear rate have focused on the wear resistance of coatings where clearly, the material being worn is also changed. Vierneusel et al [6] explored the links between residual stresses and coating wear in molybdenum disulphide, observing significant reduction in wear in specimens with coatings with a large compressive residual stress state.

1.3. Wear in externally loaded components

Naga et al [7] conducted tests with a contact geometry and loading similar to that studied in this paper but with brass, concluding that the wear rates of brass were accelerated by the presence of static tensile loads. Upon review of this data, any effect is small and inconsistent, with no data given for variability. Ho et al [8] studied the effect of residual stresses imposed by shot peening on wear rates of steels, concluding that the residual stresses created by the wear mechanisms themselves often exceed the magnitude of any pre-existing stress, therefore 'washing them out'. Ho measured *wear induced* axial stresses of 600 - 800 MPa, and shear stresses of up to 125 MPa but negligible stress perpendicular to the surface. He argued that only if the contact stresses induced were below the magnitude of the pre-existing stress state, could the pre-stressing influence the wear rate.

Owing to the number of compounding effects known to influence wear rates in metals, it is infeasible to quantify empirically the effects of changes in any single variable relative to all others. This paper simply explores whether external loading (stress due to sources other than contact loading) in a component has any significant effect on wear rate for fretting steel-steel contacts, so that it can be identified as a potential modelling requirement. The type of contact studied here was a dry (unlubricated), steel-on-steel contact as these have been thoroughly studied in the literature due to their obvious industrial prevalence. Initially, contacts of this nature wear quickly by severe mechanisms such as abrasion or adhesion, after which the wear rate slows as more mild mechanisms such as oxidation become dominant [9], [10]. In the experiments to be described, measurements of worn volume are taken cycle by cycle, so the wear rates resulting from the various mechanisms can be measured independently (as opposed to tests in which one measurement is taken at the end, and so the 'rate' calculated is an average). Consequently, the influence of external loading can be seen for each of these wear regimes (or mechanisms).

In this paper we describe the results of an experiment in which constant external loads are imposed on the specimen being worn. Experiments have been designed to apply either axial stress or torsion to cylindrical specimens. Tests in which axial pre-stresses are applied

explored the possibility that the wear mechanisms are crack driven. This is based on the assumption that changes in near surface direct stress will substantially impact crack growth, as discussed in detail by Susmel et al [4]. Torsional pre-stress experiments were performed to find the response of wear rates to more complex in-surface states of stress. Torsion was used as it allowed for application of high shear stresses in the surface of the material, as well as higher von Mises stresses than could be achieved with the axial loading method.

2. Method

The apparatus used for the experiments described in this paper is shown schematically in figure 2. A description and validation of this appeared in a previous paper [11], so only a brief description of the basic components and function is given here, alongside a more thorough explanation of the new features. In the previously described form, the apparatus was incapable of exerting external stresses on the specimens, and so modifications and additions were required. The maximum loads and displacements applied throughout the tests described here are shown in figure 2 (left), and the right hand image is a schematic of the key component arrangement. A more detailed annotated model of the rig is given in figure 3.

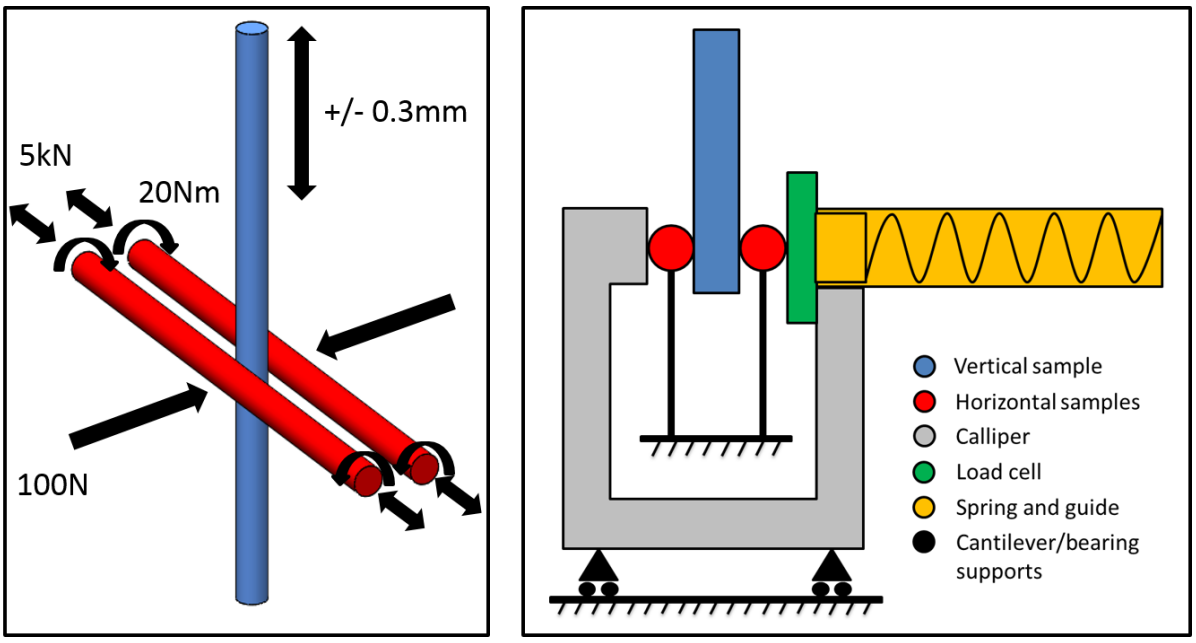

Figure 2: A diagram of the loads applied to the specimens (left) and a schematic of the key elements of the rig used (right).

2.1. Contact loading and specimen displacement

The vertical specimen (blue in figure 2) is held in a fixture connected to the actuator rod via the main load cell. The actuator applies the displacement to the vertical specimen and the shear loads in the contact, which are measured by the load cell. The fixture grips

the specimen and allows for alignment (via the differential tightening of screws) with the horizontal specimens (red). The purpose of this rig is to force the horizontal specimens onto the vertical specimen from either side to produce two, identically loaded, crossed cylinder wearing contacts. To do this, the horizontal specimens must be free to advance towards each other to maintain the contact load as material is worn away, but must also be stiffly supported in the vertical direction to react-out the shear forces in the contact. This was achieved by mounting the horizontal specimen clamps on thin, wide cantilevers, which have the required stiffness / compliance (labelled in figure 3 as 'support cantilevers').

The normal load is applied to both of the contacts by a loading caliper. This caliper rests on bearings and is free to 'float' in the direction of the applied force. Consequently, the load is identical in both contacts to within the negligible rolling friction of the bearing. The force is applied by a preloaded spring, which rests in a guide. The amount of preload can be adjusted by a screw on the back end of the guide. This load can be measured directly by a bespoke pancake load cell, located on the opposite side of the caliper from the spring. As the contact wears and the spring advances, the load applied reduces. The load cell reading was monitored throughout every test to ensure that it remained in a +/- 1% range about the nominal value. The distance through which the spring advanced was used to estimate for the worn volume, as a function of cycle number. This distance (which is equal to the change in separation of the two horizontal specimens) was measured by a linear variable differential transformer (labelled 'Local LVDT'). The next step was to find the worn volume as a function of this linear measurement. A set of tests was performed, in which the final cycle count was varied from 50 to 10000. The worn volume for each of these scars was measured using a 3D profilometer and plotted against the corresponding linear measurements. The resulting interpolated function was used to estimate the volume as a function of the LVDT measurement in future tests. The method by which the worn volume was obtained from this measurement is given in detail in the previous work [11].

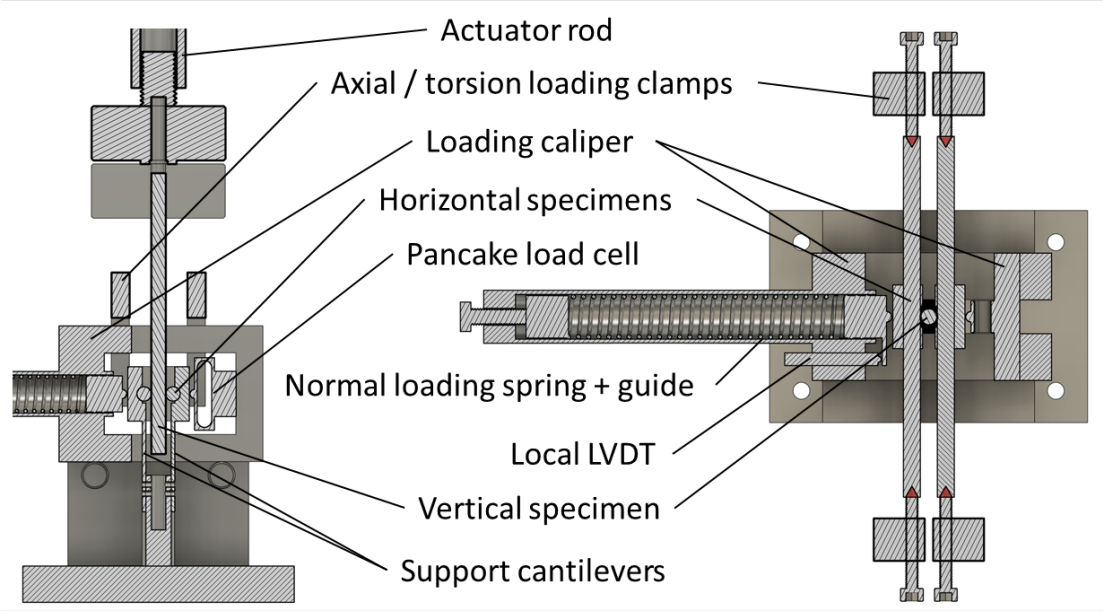

Figure 3: A labelled CAD model of the rig, with sections displaying a front view (left) and a plan view (right).

2.1.1. External loading clamps

For these tests, the rig was modified with the addition of clamps (labelled 'Axial / torsion loading clamps' above) to allow an external load to be imposed on the horizontal specimens to be worn. The cylindrical horizontal specimens were pre-loaded in three different static ways in various experiments, as follows: 1) Axial compression 2) Axial tension 3) Torsion. A set of clamps, shown in figures 3 and 4, were designed and employed to apply these loads.

1. Axial compression was applied by screws which passed through threaded holes in the clamps, and pressed into centres drilled into the ends of the specimens.

2. Axial tension was applied in a similar way, except the holes in the clamps were clearance for the screw size used, and the specimens were given a female thread and a screw applied tension.

3. Torsion was applied by a pair of levers placed at opposite ends of the clamp, which acted on 1.5 mm deep flats machined onto the specimens. Both levers were fixed in this way, relative to the specimen. One of the two levers was fixed relative to the clamp, whilst the other was free and could be forced away from the clamp by a screw, applying torsion to the specimen.

The *amount* of load applied was measured using one of two strain gauges, depending on the type of loading. Axial loading was measured using a strain gauge on the spine of the clamp. This was calibrated with a tensile testing machine with a professionally calibrated

load cell. Torsion was measured using a gauge on the lever used to apply load, and a calibration was performed by hanging a known mass at a distance from the specimen. A model of the complete assembled rig as it was used for the tests described in this paper, is shown in figure 5.

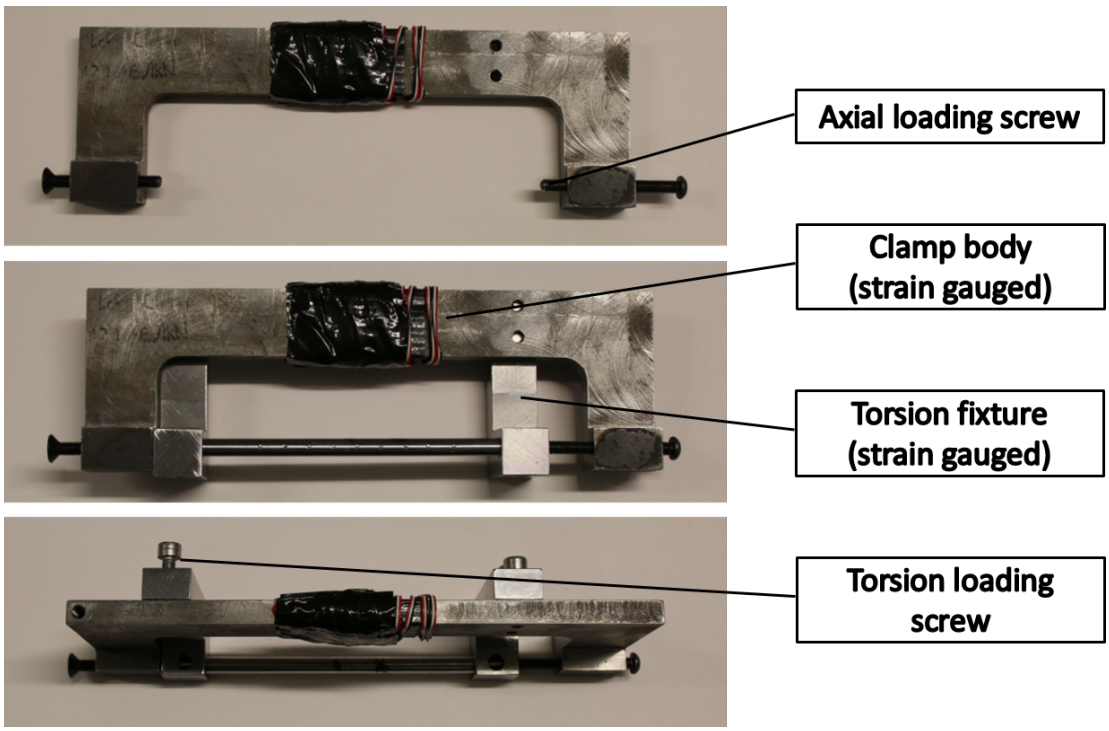

Figure 4: The bespoke clamps used to apply external loads in the specimen. These images show the mechanism by which the torsion was applied to specimens, through 2 levers acting on a ground flat on the specimen.

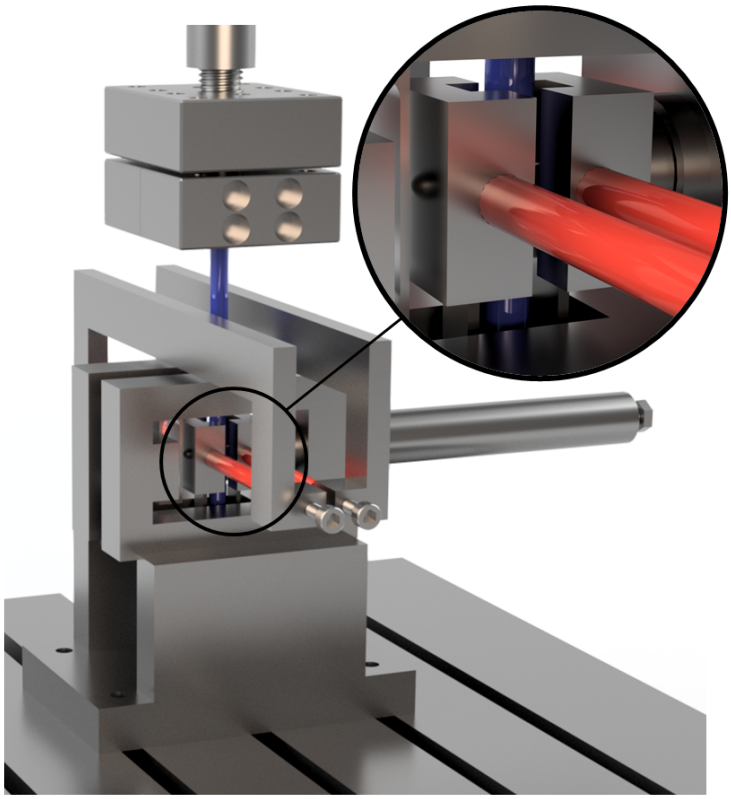

Figure 5: A CAD render of the apparatus in the fully assembled form. The vertical and horizontal specimens have been coloured blue and red respectively.

2.2. Test parameters

The EN24-T steel used in these tests is typically chosen for its wear resistance after heat treatment, and was supplied (by Steel Express, Wolverhampton, UK [12]) in 10 mm diameter rods containing 0.44% C, 0.35% Si, 0.7% Mn, 0.04% S, 0.035% P, 1.4% Cr, 0.35% Mo, 1.7% Ni. Experiments were run for 10,000 cycles, at 5 Hz, over which duration gross frictional heating of the contact was found to be negligible. Each specimen was turned on a lathe to around 8.3 mm and then ground to 8 +/- 0.005 mm, and to a roughness value of 0.3 µm Ra, measured on an Alicona G4 Infinite focus Optical 3D profilometer. All specimens were cleaned with acetone to remove any manufacturing or handling contaminants, immediately before each test. The normal load in all tests described here was 100 N, and the displacement amplitude in the contact was 0.3 mm.

A wear experiment was performed for each type of external loading (compression, tension, torsion). For each experiment, the tests were conducted at two (or in the case of torsion, three) values of the chosen external load type. Tests with zero external load had been conducted previously, but additional control tests were performed in this study to allow for the dynamic effects of the presence of the clamps, and to isolate the effects of the additional external load. In these control tests, a relatively small external load was applied to the

specimen to give it the same dynamic response. The loads applied in the tests were as follows:

1. Axial compression - a) 20 MPa control b) 100 MPa maximum.

2. Axial tension - a) 20 MPa control b) 100 MPa maximum.

3. Torsion - a) 5 Nm b) 10 Nm c) 20 Nm.

The number of tests performed for each experiment varied due to specimen availability and control / hydraulic failures during tests. At least 3 complete tests in each configuration were achieved.

3. Results

3.1. Experimental results

Results are given here for all 31 tests completed. Figures 6, 7, and 8 show plots of worn volume vs cycle number for the tests from the compression, tension and torsion experiments, respectively. Each plot shows both the high value and control value for that mode of external loading.

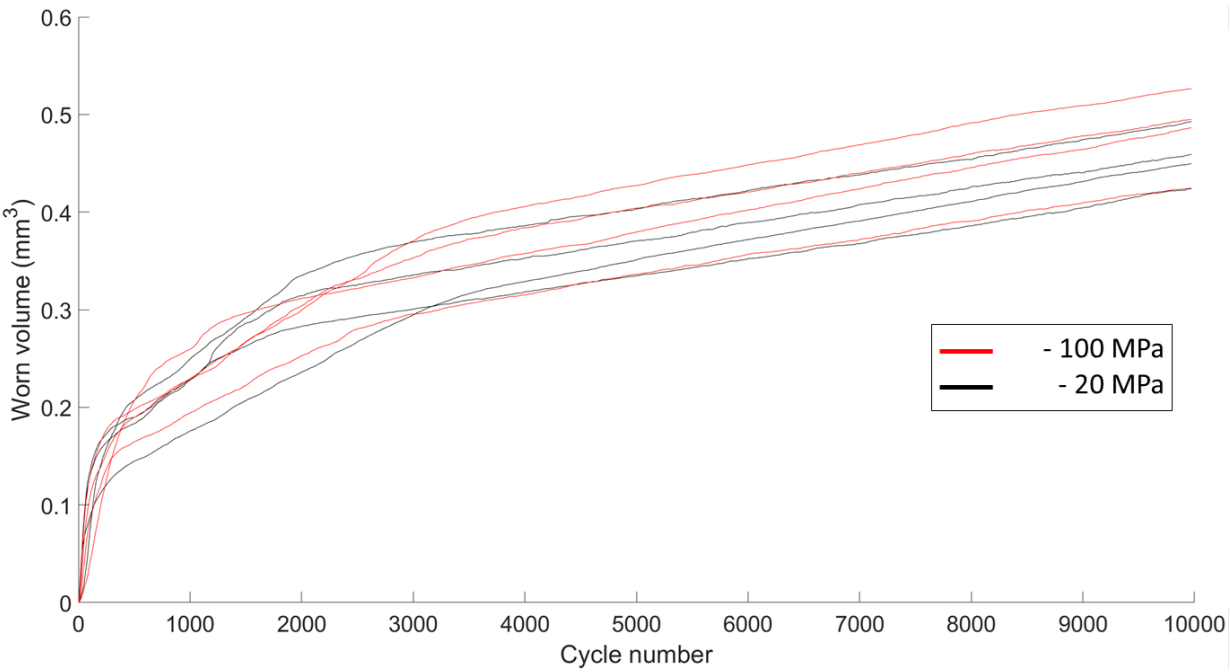

Figure 6: Graphs of the worn volume vs cycle data in the 4 control (20MPa) and 4 full load (100MPa), compression tests

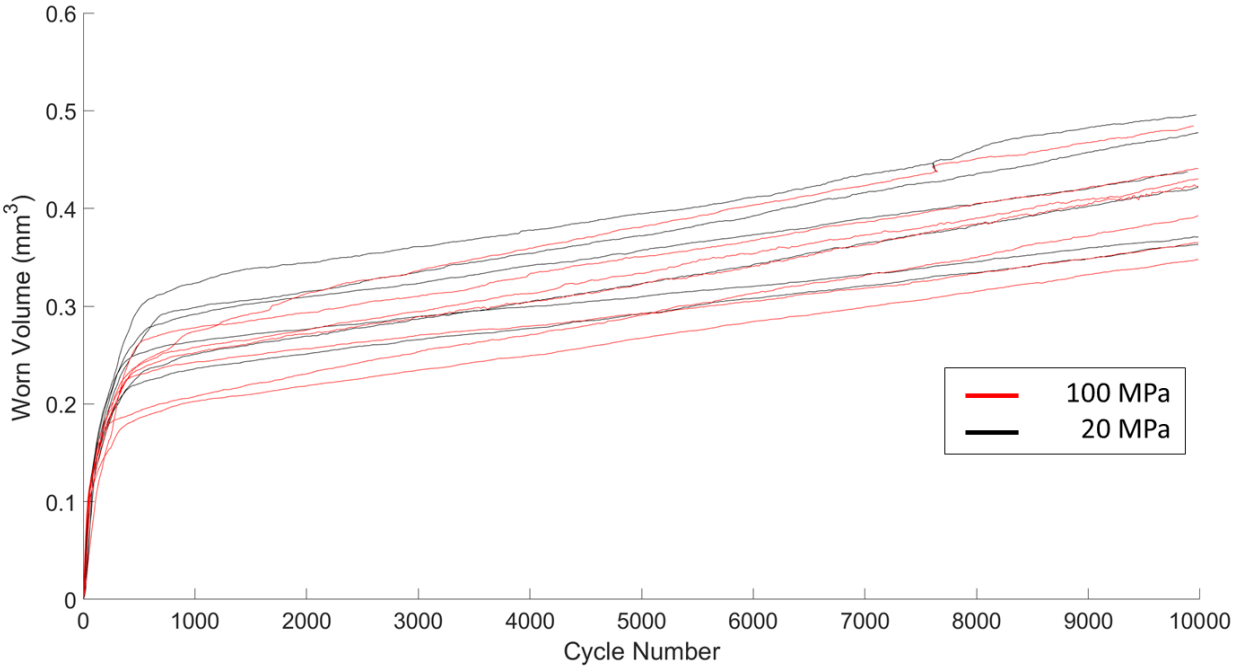

Figure 7: Graphs of the worn volume vs cycle data in the 6 control (20MPa) and 7 full load (100MPa), tension tests

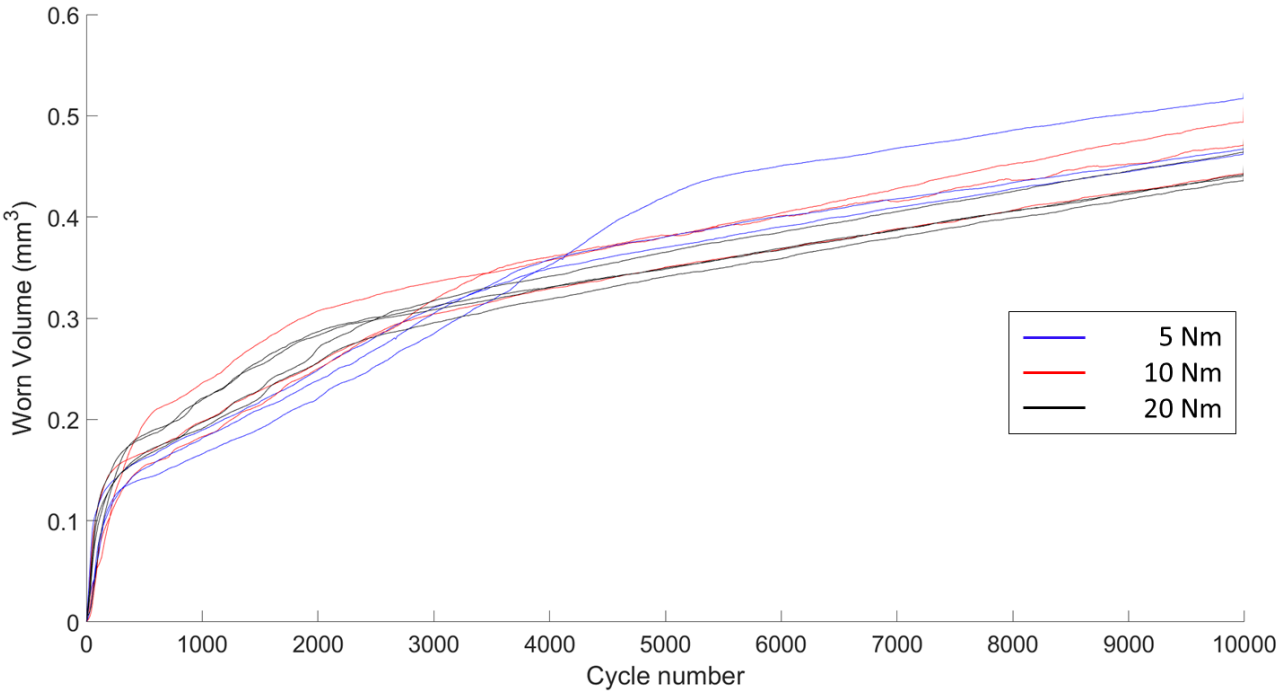

Figure 8: Graphs of the worn volume vs cycle data in the 3 low load (5 Nm), 3 medium load (10 Nm) and 4 high load (20 Nm) torsion tests

First, whilst acceptable spread is difficult to quantify, the repeatability observed for all tests was considered acceptable for the identification any strong effects of the application of external load on wear rate. No consistent qualitative difference was observed between the results of tests within the same experiment (or external loading type). Any variation between tests carried out at different parameters was significantly *smaller* than the variation within tests of the same parameters.

All graphs presented here are approximately bilinear in shape, which is typical for the wear of unlubricated steels in air [9]. Some tests (particularly results from compression and torsion tests) exhibit a three-gradient shape. All tests bar one exhibited a constant wear rate from cycle 3000 onwards. The final worn volume (at cycle 10000) for all tests is around 0.4 - 0.5 mm^3. For each mode of loading, the overlap of 'control' and 'full load' data indicates that there is *no* significant effect on total worn volume. Furthermore, considering the similarity of the gradients in both the transient (before 3000 cycles) and steady state (from 3000 cycles) data in all 3 experiments, we conclude that the external loading has no effect on any wear mechanism active in the tests (discussed further in sections 3.2 and 3.3).

The multi-gradient graphs are often interpreted as changes in wear mechanism in the literature [9], as there is a step change in wear rate without a step change in any measured parameter. The results of previously published tests, performed under identical conditions only without external load, are included here in figure 9 for the purpose of comparison. Data from from these previous tests and from the external tension experiment reported here (figures 9 and 7, respectively) exhibit bilinear wear rate graphs, whilst the data from the compression and torsion experiments (figures 6 and 8, respectively) exhibit trilinear wear rates. In all cases, the first transition occurs around the same cycle number (300-500). The second transition, if it occurs, does so in the cycle range 2000-3000. The reason for this first transition is believed to be the transition from severe to mild wear (from abrasive / adhesive wear mechanisms to oxidative mechanisms). The reason for the presence of the second slope is not known, however the function of the control tests is to separate these effects out from those resulting from changes in applied stress. In all cases, there is no repeatable difference between the control tests and the more highly loaded tests of the same type, so reliable conclusions can be drawn from each set whilst comparison between sets may be compromised.

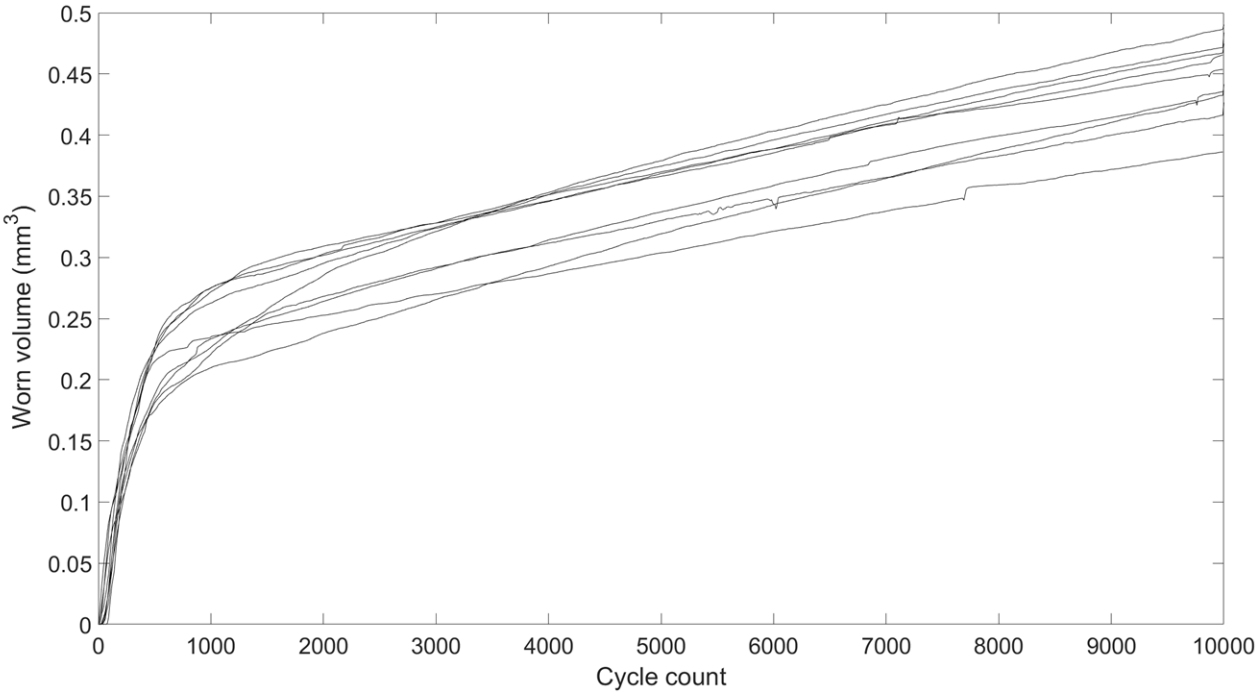

Figure 9: Graphs of worn volume vs cycle number for previously published tests, for comparison to the modified experiment presented here [11].

3.2. Effects of axial load on wear

The results of the axial load tests show clearly that for the conditions studied, neither tensile nor compressive stresses had an observable effect on the wear rate of the specimens at any cycle range, or the final worn volume. The full range of axial loads tested was 200 MPa and the yield stress of the material was 650 MPa. The significance of this result is the implication that the wear mechanisms present in this contact are not strongly crack driven, and that moderate externally applied surface stresses or residual stresses can be neglected when modelling the wear of components. The maximum possible axial loads are limited here by the clamps, but it may be the case that very large axial loadings (close to yield) would cause an important change in wear rate.

3.3. Effects of torsional load on wear

A much larger change to von Mises' stress was achievable through the application of torsional loads, than was by axial loads, so these tests are more appropriate to assess the role of plasticity in the present wearing mechanisms. Tests were conducted with horizontal specimens subjected to 5, 10 and 20 Nm of torsion, and no significant change in wear rate was observed. The von Mises stress in the contact due to the normal and shear loads is impossible to calculate with any certainty, as the contact is only well defined initially (before wear); the wear scars are very complex in their geometry. The area of the contact region changes with wear due to the geometry of the specimens, but is known to vary from 0.7 to 7 mm^2 determined by methods described in the methods section of this paper and more completely

in a previous paper [11]. The corresponding nominal (assuming uniform distribution of normal and shear loads) von Mises stresses in the contact, given a 100 N normal load and an assumed coefficient of friction of 0.7, vary from 230 MPa (initial) to 30 MPa (final), with contact area development. The von Mises stress in the specimens, resulting from torsion loads, was found by finite element analysis (FE) due to the complex geometry. A wear scar was incorporated into the model, as it raises the local stress due to its geometric effect and significant reduction of cross sectional area over which the torsion can be carried. This scar was modelled simply as a circular cut from the specimen, perpendicular to the axis of the specimen, as shown in figure 10 (left). Two cases were modelled, one at minimum and one at maximum scar size (start and end of a test), both at 20 Nm torque. Figure 11 shows the results of these two models. Outside the scar, a von Mises stress of 340 MPa was found, and the values at the centre of the scar were 370 MPa and 440 MPa for the minimum and maximum scar sizes respectively. Considering the relative effects on von Mises stress of the contact loads and torsion, it could be argued that at the start of the test (small scar size), the effects are similar (230 MPa and 370 MPa respectively). However, considering a larger wear scar as observed in the latter half of the test (5000 cycles onwards), the contribution of the torsion to von Mises stress (440 MPa) is much greater than that of contact stresses (30 MPa). The lack of change of wear rate with torsion application therefore strongly indicates that on a macro scale (in contrast to an asperity scale) plasticity is unlikely to be strongly linked to the wear mechanisms present. The EN24-T steel specimens had a 0.2% yield stress of 650 MPa, which is less than 150% of the maximum von Mises stresses induced by external torsion loading. Furthermore, the choice of crossed cylinder geometry results in a wearing contact which is initially formed through yielding. Since the change in von Mises stress in the contact during the steady state cycle band is increased by the external loading clamps by an amount greater than the contact loads, the authors consider the torsion applied to be sufficient to study this effect.

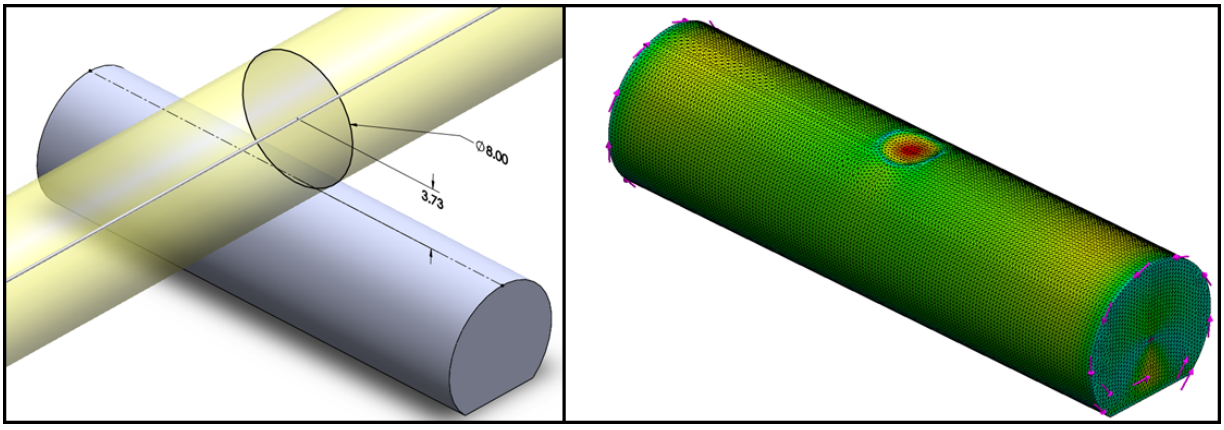

Figure 10: CAD modelling of an approximate wear scar for analysis of the change in von Mises stress due to the application of torsion loads (left). Finite element model result with von Mises contour plots (right)

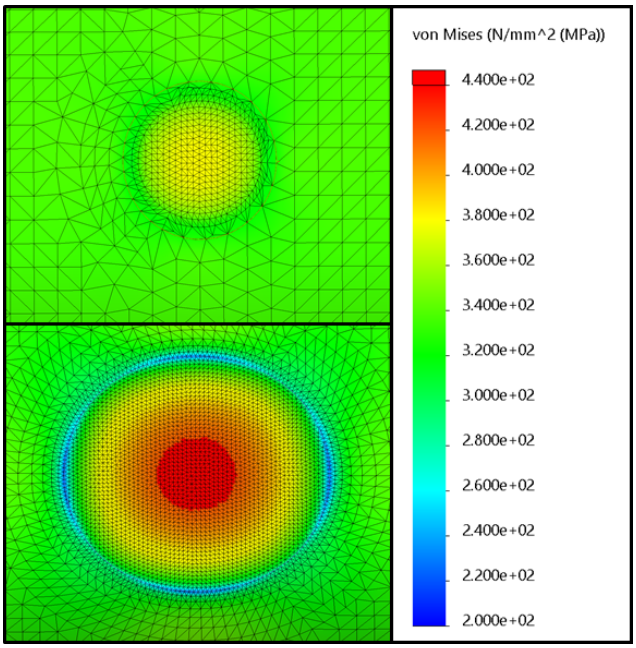

Figure 11: Finite element contour plots of von Mises stress in the wear scar of approximately minimal (top) and maximal (bottom) sizes

3.4. Comparison with literature and implications for wear modelling

Comparison of the results of any wear test to those in the literature is difficult for any study considered, as experiments vary in at least one key variable known to affect wear rate. There are also very few studies of external loading in wear. The work of Naga et al [7] claims an effect of external stress on wear rate in brass, which was not observed in our results. Upon review, the Naga results exhibit only a very small effect, if any, and the claimed effect of external load on wear is not consistently monotonic. In that sense, their results and those presented here are in agreement; what might be small effects are hidden by noise. Our previous work [11] indicated that in the steady state wear regime (after 2000 cycles), the debris particles ejected are 100% oxide. It is possible that the external stresses have no effect on the wear of steels in the steady state in this experiment because the main mechanism is oxidation, which is not stress dependent.

Whilst oxidative wear mechanisms explain the insensitivity of wear rate to this external load in the steady state condition, the wear rates in the transient stage of the tests (the first gradient, typically before 2000 cycles) are similarly insensitive. As shown in the previous work [11], the debris produced in this transient stage is almost entirely metallic, and could not be produced by oxidative wear mechanisms. As suggested in section 1.3, an explanation offered by Ho et al [8], is that the residual stresses induced in the contact exceeded the applied external stresses and so subsequent wear is uninfluenced. The following section explores this hypothesis.

3.5. Modelling of surface residual stress

A second FE model was produced to find the effects of plasticity on the stress state in the contact interface and the effects of the external loading on this plasticity. To simplify the problem, and to allow the use of a more refined mesh, a 2D plane strain model was used, in which the peak pressure was matched to the experimental geometry. Kinematic hardening plasticity, using experimental data for EN24-T from [13], was enabled. The model is shown in figure 12, with annotated boundary conditions. The displacement range was run for 3 cycles and then the contact was separated, leaving only the plastic residual stresses. This model was run for two conditions. First, without any external load, and then with a 300 MPa tensile external load (approximately representative of the von Mises stress changes in the torsional experiments), applied to the upper specimen in the axial (through plane, Szz) direction. In order to apply a stress in the through plane direction, the upper body was given anisotropic thermal expansion properties, such that for the applied temperature change, a through plane stress of 300 MPa could be developed.

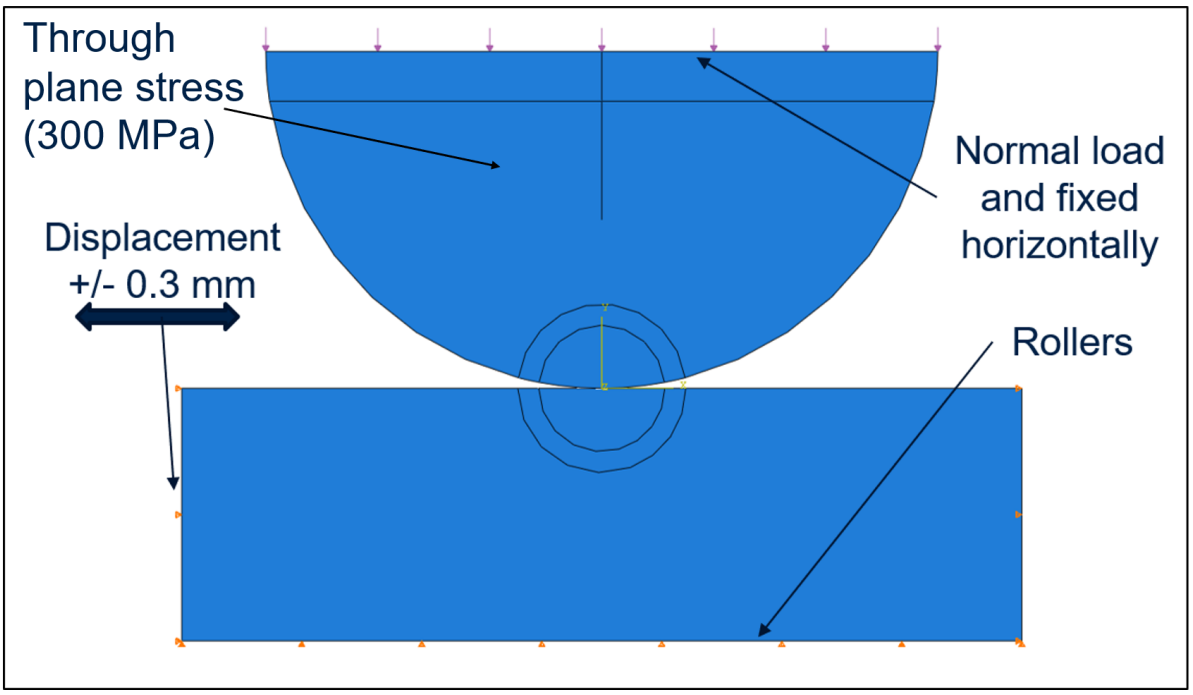

Figure 12: Diagram of the FE model used to explore the residual stresses

The required output of the modelling was the stress (in the axial direction (Szz)) at the surface of the upper specimen, for the unloaded and externally loaded cases. This result is given below in figure 13. This graph shows clearly that plastic residual stresses which accumulate in the contact, even after just 3 cycles, are sufficient to counteract even substantial external loading. Distant from the contact, the difference in stress tends toward the external loading value of 300 MPa as expected. Within the contact, the maximum difference between the two cases the is just 50-100 MPa. The largest differences can be

seen right at the edges of contact, which are the regions to see the smallest amount of local plasticity, as they have the smallest proportion of time in contact per cycle. The difference in Szz at positions well within the contact is just 10 - 20 MPa. It is concluded that the suggestion offered by Ho et al is correct, explaining the insensitivity of wear to external loading.

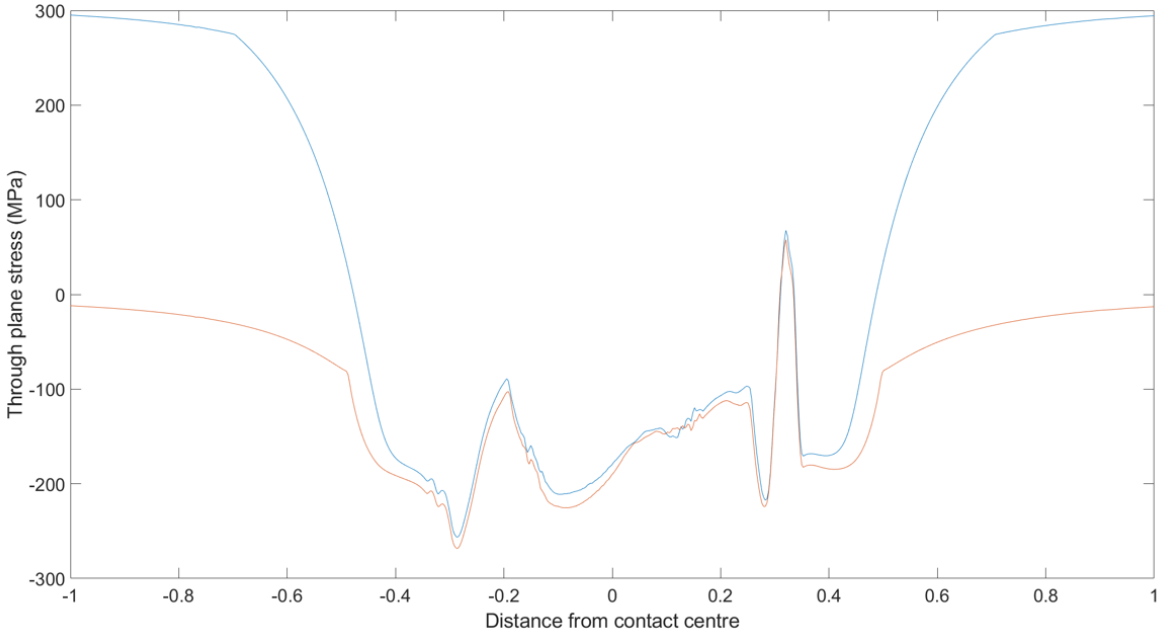

Figure 13: Through plane stress (σzz) at the contact following 3 loading cycles

4. Conclusions

Cylindrical wear specimens were arranged in a crossed cylinder configuration and a relative displacement was applied to produce a wearing contact, in which the wear rate could be measured as a function of cycle number. Fixtures were designed to enable the application of three types of external loading to the static specimens: compression, tension and torsion. An analysis was performed, and it was shown that the applied external loads caused substantial changes to the von Mises stress in the contact, relative to the von Mises stress resulting from the contact loads. From the results presented here, it can be concluded for each of the external loading modes considered (tension, compression and torsion) and at the load levels applied, no significant changes to wear rate were observed.

The implication of the 'axial stress' results, is that the wear mechanisms present are not crack growth dominant. If they were, axial compression would be expected to suppress wear and tension would be expected to exacerbate it, in agreement with modified Goodman diagrams and the like [14]. Similarly, the constant wear rate across tests with a widely varying von Mises stress in the contact, indicates that plasticity is not dominant in the removal of

material from the contact for these mechanisms - there are stronger rate-determining factors. These factors might include the oxidation rate of the material, or the ejection rate of the debris, which would be unaffected by the stress state of the substrate material. That said, subsequent analysis showed that because of the degree of plastic deformation around the contact due to contact loading in the transient stage (when the contact is very small and the pressure is high), the presence of a significant external load makes no difference to the local stress field, explaining the insensitivity of wear rate in this cycle range. Note that this remark only applies when the contact is plastically dominated, and the previous remarks about the effects of the external load on contacts wearing by oxidative mechanisms are still valid. This is because the contact loads are within the elastic limit (macroscopically) during the steady state.

This has an important consequence to any effort to model wear in highly stressed components - that wear rates are determined primarily by contact stresses and the more general stress field can be disregarded in all but the more extreme cases of external loading.

5. Acknowledgements

The authors are grateful to Rolls-Royce plc for providing the financial support for this project and for giving permission to publish this work. This work is part of a Collaborative R&T Project 'SAGE 3 WP4 Nonlinear Systems' supported by the CleanSky Joint Undertaking and carried out by Rolls-Royce plc and the University of Exeter.

References

[1] O. Vingsbo and S. Söderberg, "On fretting maps," *Wear*, vol. 126, no. 2, pp. 131–147, 1988.
[2] J. Archard, "Contact and rubbing of flat surfaces," *Journal of applied physics*, vol. 24, no. 8, pp. 981–988, 1953.
[3] H. Andresen and D. Hills, "A review of partial slip solutions for contacts represented by half-planes including bulk tension and moments," *Tribology International*, vol. 143, p. 106050, 2020.
[4] L. Susmel, R. Tovo, and P. Lazzarin, "The mean stress effect on the high-cycle fatigue strength from a multiaxial fatigue point of view," *International Journal of Fatigue*, vol. 27, no. 8, pp. 928–943, 2005.
[5] Z. Lin, Z. Wang, and X. Sun, "The influence of internal stress and preferred orientation on the abrasive wear resistance of a boronized medium carbon steel," *Wear*, vol. 138, no. 1-2, pp. 285–294, 1990.
[6] B. Vierneusel, L. Benker, S. Tremmel, M. Göken, and B. Merle, "Isolating the effect of residual stresses on coating wear by a mechanical stress relaxation technique," *Thin Solid Films*, vol. 638, pp. 159–166, 2017.
[7] S. Naga, S. Riad, M. Mokhtar, and E. Gewfil, "Wear failure as influenced by external stressing," *Wear*, vol. 145, no. 2, pp. 297–302, 1991.
[8] J. Ho, C. Noyan, J. Cohen, V. Khanna, and Z. Eliezer, "Residual stresses and sliding wear," *Wear*, vol. 84, no. 2, pp. 183–202, 1983.
[9] J. Archard and W. Hirst, "The wear of metals under unlubricated conditions," *Proc. R. Soc. Lond. A*, vol. 236, no. 1206, pp. 397–410, 1956.
[10] F. Stott and G. Wood, "The influence of oxides on the friction and wear of alloys," *Tribology International*, vol. 11, no. 4, pp. 211–218, 1978.
[11] L. Blades, D. Hills, D. Nowell, K. E. Evans, and C. Smith, "An exploration of debris types and their influence on wear rates in fretting," *Wear*, p. 203252, 2020.

[12] STEELEXPRESS, "EN24T Steel Properties." http://www.steelexpress.co.uk/engineeringsteel/EN24T-properties.html. Online; accessed 12 October 2017.
[13] N. Bharat and K. Chakraborty, "Machinability of en 24 steel (817m40),"
[14] J. Schijve, *Fatigue of structures and materials*. Springer Science & Business Media, 2001.